Microscopy and Microanalysis, 2023, **00**, 1–15
https://doi.org/10.1093/micmic/ozad050

Microscopy AND Microanalysis

Original Article

A New Method for Dead Time Calibration and a New Expression for Correction of WDS Intensities for Microanalysis

John J. Donovan[1,*], Aurélien Moy[2], Anette von der Handt[3], Zack Gainsforth[4], James L. Maner[5], William Nachlas[2], and John Fournelle[2]

[1]*CAMCOR, University of Oregon, 1443 East 13th Ave, Eugene, OR 97403, USA*
[2]*Geoscience Department, University of Wisconsin-Madison, 1215 W Dayton St, Madison, WI 53706, USA*
[3]*EOAS, University of British Columbia, 2207 Main Mall #2020, Vancouver, BC V6T 1Z4, Canada*
[4]*Space Sciences Laboratory, University of California at Berkeley, 7 Gauss Way, Berkeley, CA 94720, USA*
[5]*Nuclear Materials Science Group, Materials Science and Technologist Division, Los Alamos National Laboratory, PO BOX 1663, Los Alamos, NM 87545, USA*

***Corresponding author:** John J. Donovan, E-mail: donovan@uoregon.edu

Abstract

Observed photon count rates must be corrected for detector dead time effects for accurate quantification, especially at high count rates. We present the "constant *k*-ratio" method, a new approach for calibrating dead time for wavelength dispersive spectrometers by measuring *k*-ratios as a function of beam current. The method is based on the observation that for a given emission line at a specific take-off angle and electron beam energy, the intensity ratio from two materials containing the element should remain constant as a function of beam current, if the dead time calibration is accurate. The method has the advantage that it does not rely on the linearity of the beam current picoammeter, yet also allows the analyst to evaluate the picoammeter linearity, another critical parameter in EPMA calibration. By simultaneously comparing *k*-ratios for all spectrometers, one can also ascertain *k*-ratio consensus, essential for inter-laboratory comparisons. We also introduce improved dead time expressions and provide best practices on how to perform these instrument calibrations using this new "constant *k*-ratio" method. These improvements enable quantitative analysis of major and minor elements with high accuracy at high beam currents, simultaneously with trace elements with high sensitivity, for point analyses and X-ray mapping.

Key words: constant *k*-ratio, dead time, EPMA, high speed mapping, WDS

Introduction

The most commonly used X-ray counting system in wavelength dispersive spectrometers (WDS) in electron probe micro-analyzers (EPMA) is the gas proportional counter and its associated electronics. This detector type covers a wide range of X-ray energies and has an excellent dynamic range for count rates typically attained in the past. In the last decade or so, a new generation of large area Bragg diffraction crystals can yield significantly higher WDS count rates than previously attained. These larger Bragg crystals have improved measurement precision and throughput, however, these increased count rates also stress our traditional dead time correction model, especially at analytical conditions utilized in major/trace element analysis and quantitative X-ray mapping (Donovan et al., 2021). At these higher count rates, the traditional dead time correction expression can quickly lose accuracy, which directly affects our corrected intensities, leading to significant errors in quantification. We will discuss the physics behind our dead time expressions, how to calibrate dead time constants using the proposed "constant *k*-ratio" method, and best practices to utilize improved dead time expressions in quantitative WDS X-ray microanalysis.

The measurement of X-rays requires consideration of photon coincidence, a phenomenon that occurs when X-rays arrive at the detector faster than it is capable of discriminating them and is often referred to as "dead time". Photon coincidence in a WDS system can arise from the physics of the X-ray counter and/or response of the electronics pulse processing system, and due to the random nature of photon production, requires proper characterization of multi-photon counting events. X-ray coincidence in WDS is typically corrected using a software based dead time correction of the observed WDS intensities for a fixed counting interval. This is in contrast to dead time corrections for energy dispersive spectrometry (EDS) systems, which utilize hardware electronics to extend the acquisition time to account for these dead time effects. Although, there have been various attempts to provide a hardware based correction for WDS dead time, see particularly Geller & Herrington (2002) and Kato et al. (2018), there has been little recent effort to improve the software based dead time correction of WDS intensities.

The WDS detector and downstream electronics processing dead time reflect the amount of time required to completely detect, process, and count a single incident X-ray photon. At sufficiently high count rates, it is possible for a subsequent photon to arrive during this interval; therefore, this photon is not observed during the "live time" integration period and hence not counted. At even higher count rates, two or more coincident

Received: January 11, 2023. **Revised:** March 20, 2023. **Accepted:** April 13, 2023

Table 1. Comparison of the Traditional Dead Time Expression with Random Photon Statistics, Following a Poisson Distribution, from Monte Carlo Simulations Assuming a Dead Time Interval of 2 μs Demonstrating that the Traditional Dead Time Expression Properly Accounts for Single and Multiple Photon Coincidence Events. We Simulated the Dead Time of a Detector with a Number of Steps N Equal to 300,000,000, a Time Interval T_i of 100 ns (Twenty Times Smaller than the Dead Time). The Total Simulated Time was 30 s. The Count Rate N of Emitted Photons was Varied from 10 cps to 400,000 cps and the Number of "Observed" Photons Recorded Accordingly. For Comparison, the Traditional Dead Time Correction Expression was also Used to Calculate the Number of Predicted Photons. In Addition, the Number of Single, Double, and Triple Photon Events Detected within Each Dead Time Interval was Calculated, and Expressed as a Percent of the Total Events at Count Rates from 10 cps to 400 kcps.

Traditional (2 μs)		Monte Carlo (2 μs)							
Predicted	Observed	Predicted	Observed	Number of single photons	Percent single photon events	Number of double photons	Percent double photon events	Number of triple photons	Percent triple photon events
10	10	10	10	9,999,795	100.0	205	0.0	0	0.0
100	100	97	97	9,998,003	100.0	1997	0.0	0	0.0
1000	998	1008	1008	9,980,060	99.8	19,923	0.2	17	0.0
10,000	9804	9978	9782	9,802,442	98.0	195,575	2.0	1969	0.0
100,000	83,333	99,965	83,347	8,186,933	81.9	1,637,694	16.4	163,922	1.6
200,000	142,857	199,897	142,787	6,703,842	67.0	2,681,098	26.8	536,106	5.4
400,000	222,222	400,318	221,948	4,492,436	44.9	3,594,378	35.9	1,438,583	14.4

photons can similarly arrive within this same dead time interval and also not be counted. To correct for these single and multiple coincident missing photons, we must perform a correction in the software for WDS X-ray counting systems. We can describe the correction of these WDS dead time effects as "nonextending" dead time corrections since the spectrometer "live time" is not extended during these dead time intervals.

These dead time effects can occur in several places within the detector and pulse processing electronics. Missing photon counts can result from various interactions of these short duration pulses inside the detector due to the ionization time of the detector gas, within the pulse processing electronics due to the intrinsic resistance and capacitance of the pulse processing and digitization circuits in various ways depending on the specifics of these electronic components which vary from manufacturer to manufacturer and model year to model year. The exact electronic details are not important, but it is important that we recognize these cumulative pulse production and processing effects, all of which fall under the general term of dead time, and that we properly correct for these effects to allow for accurate quantitative analyses over a wide range of count rates.

The Linear Dead Time Expression

The traditional form of the dead time expression is commonly notated as

$$I_{\text{cps}} = \frac{i_{\text{cps}}}{1 - (i_{\text{cps}} \cdot \tau)} \quad (1)$$

where: I_{cps} is the dead time corrected (predicted) count rate in cps, τ is the dead time constant in seconds, and i_{cps} is the raw (observed) count rate in cps.

This classic linear expression (Goldstein et al., 1992, Ruark & Brammer, 1937, p. 289) has been utilized for decades for the correction of observed WDS intensities. It is also traditionally used for determination of the WDS dead time constants. This equation considers the mathematical probability of a photon coincident within the dead time interval of the spectrometer system with an initial incident photon. The equation further assumes that the photon pulse shape is mathematically rectilinear and that the dead time interval is constant as a function of count rate. In fact, with these assumptions, the traditional form of the dead time correction properly handles not only single photon coincidence events but also multiple coincidence photon events.

This can be seen by performing Monte Carlo simulations of photon emission following a Poisson distribution and counted by a detector with a perfect pulse shape and constant dead time, as shown in Table 1. We can see that the traditional dead time expression yields almost identical results when compared to the Monte Carlo simulations for a nominal dead time interval of 2 μs, a common value for WDS X-ray counters, though any dead time constant value can be modeled with similar results. The details of the Monte Carlo simulation, source code and simulation results as an Excel file, are noted in the Appendix and included as supplementary files.

We conclude from these Monte Carlo results that when the pulse widths are sufficiently distinct in time and rarely overlap, the behavior of the WDS system is essentially linear in response, and the dead time effects are well described by the traditional dead time expression. Because of this assumption of an exactly rectilinear pulse shape and constant dead time relative to the count rate, the traditional dead time expression is limited to input count rates up to ~50 kcps; a region in which the dead time pulse processing effects are minimal compared to the average time between the pulses and yield a fairly linear response with beam current. However, as the pulses begin to overlap in time at sufficiently high count rates due to the imperfect pulse shapes as observed in typical pulse processing electronics (Geller & Herrington, 2002), at count rates higher than ~50 kcps, these nonideal pulse shapes begin to become similar to the average time between photon pulses and therefore, start to impact the accuracy of the traditional dead time model. In addition, it is possible that the assumption of a constant dead time interval at higher count rates is not perfectly valid (i.e., an extending dead time constant) (Beaman & Solosky, 1972). We therefore must precisely characterize these nonlinear dead time artifacts to improve modeling for accurate quantitative analysis at these higher count rates.

In addition to the above considerations, the linearity of the picoammeter is also critical for accurate estimates of raw or "observed" count rate versus beam current as utilized in traditional determinations of dead time constants. In fact, Heinrich et al. (1966) proposed a "ratio" method for the determination of dead time that was based on the measurement of simultaneous Kα and Kβ emissions on two spectrometers,

thereby eliminating any nonlinearity of the picoammeter. However, the Heinrich "ratio" method still assumes a linear response of the pulse processing system which is problematic. We therefore propose a new nonlinear expression for an improved software correction of WDS intensities for dead time effects. In addition, we also propose a new method for determining the accuracy of our dead time constants, which utilizes the ratio of two intensities from two materials, which we call the "constant *k*-ratio" method. Simply because the traditional WDS *k*-ratio should (ideally) remain constant as a function of beam current, if the dead time correction is being properly applied in software.

Expressions for Nonlinear Dead Time Correction

A significant improvement in dead time correction accuracy at these higher count rates has been described by the use of an additional term in the traditional linear expression as shown here from Willis et al. (1993).

$$I_{cps} = \frac{i_{cps}}{1 - \left(i_{cps} \cdot \tau + i_{cps}^2 \cdot \frac{\tau^2}{2}\right)} \quad (2)$$

This nonlinear expression was originally developed for calculating work function "dead time" for training of early neural networks but has now been applied to microanalysis and found useful for correction of observed count rates up to roughly 100 kcps, as we will demonstrate below. These are count rates often encountered when using moderate to high beam currents and/or when dead time constants are larger than 2 µs. This Willis expression has been sufficient for most EPMA work until the recent introduction of large area Bragg crystals on newer EPMA instruments which yield considerably higher X-ray intensities for a given beam current.

Upon recognizing that the Willis expression is merely the first two terms of an infinite Maclaurin expansion series, where each additional term more accurately describes the effects of nonlinear pulse processing effects with decreasing time between the pulses, we can simply increase the number of infinitesimal terms to effectively deal with even higher count rates.

Therefore, we propose a new dead time correction expression which should be utilized if count rates exceed 100 to 200 kcps (depending on the exact value of the dead time constant). This new expression is again merely an extended form of this Maclaurin like expansion series as shown here, with an additional four terms of the series to further improve modeling of these nonlinear dead time effects (further increasing the number of terms has essentially little to no effect even at these high count rates):

$$I_{cps} = \frac{i_{cps}}{1 - \left(i_{cps} \cdot \tau + i_{cps}^2 \cdot \frac{\tau^2}{2} + i_{cps}^3 \cdot \frac{\tau^3}{3} + i_{cps}^4 \cdot \frac{\tau^4}{4} + i_{cps}^5 \cdot \frac{\tau^5}{5} + i_{cps}^6 \cdot \frac{\tau^6}{6}\right)} \quad (3)$$

Such high count rates are quite readily obtained at even moderately high beam currents when utilizing modern instruments with large area Bragg diffraction crystals with strong emission lines. Though in fact, this extended form of the dead time correction expression can still be utilized at low and moderate count rates to correct for simple photon coincidence because these high-order terms are all close to zero at low to moderate EPMA count rates. Furthermore, hardware and electronics pulse processing limitations at extremely high count rates will generally restrict the application of these extended expressions long before reaching their mathematical limits, e.g., when the product of count rate and dead time exceed 1 for both the traditional linear and expanded nonlinear expressions. However, in practice, the six-term expanded expression (Eq. (3)) is applicable to trace, minor and major element WDS microanalysis from low count rates to count rates up to approximately 300 to 400 kcps depending on the actual dead time constants of the particular EPMA hardware.

Thankfully, we can greatly simplify this expression by recognizing the Maclaurin series of $\ln(1 - x)$, where ln denotes the natural logarithm:

$$\ln(1 - x) \approx -x - \frac{x^2}{2} - \frac{x^3}{3} - \frac{x^4}{4} - \ldots$$

and with $x = \tau \cdot i_{cps}$:

$$\ln(1 - \tau \cdot i_{cps}) \approx -\tau \cdot i_{cps} - \frac{\tau^2 \cdot i_{cps}^2}{2} - \frac{\tau^3 \cdot i_{cps}^3}{3} - \frac{\tau^4 \cdot i_{cps}^4}{4} - \ldots$$

hence, we have:

$$I_{cps} = \frac{i_{cps}}{1 + \ln(1 - \tau \cdot i_{cps})} \quad (4)$$

With this logarithmic expression, we can correct for not only photon coincidence at low to moderate count rates but also at higher input count rates for nonlinear response of the WDS detectors and pulse processing electronics for improved accuracy at high beam currents, which have been previously impractical for quantitative analysis. Once again, all of these new expressions yield identical results to the traditional expression at sufficiently low count rates and therefore, this logarithmic expression can be applied at low, moderate, and high beam currents (proxy for count rates). Moreover, we can now better appreciate that the so-called dead time constant is actually a *parametric* constant, because its exact value depends on the specific expression we utilize for predicting the actual count rate from our observed count rate. In practice, this means that if our original dead time constants were calibrated using the traditional linear model, we will need to slightly decrease the values of our dead time constants when utilizing these more precise dead time models, to account for improved modeling of these nonlinear effects at higher count rates. Typically, this means slightly lowering the dead time constants a few hundredths of a μs as discussed below. This is a tiny numerical change which is essentially invisible at low to moderate count rates. The appropriate dead time values to be used with these more precise dead time models should be obtained using the dead time calibration methods as detailed bellow.

At even higher count rates (>300 or 400 kcps, depending on the hardware specifics) these nonlinear effects come to dominate the pulse processing electronics, and the dead time correction becomes extremely sensitive to the exact value of the dead time constant utilized. For example, some instruments multiplex the pulse pileup processing from multiple spectrometers into a single circuit, while other electronic processing delays can become more relevant when pulse streams approach the frequency of the response time in the processing electronics.

Regardless of pulse processing limitations, it might be appropriate to utilize an even more radical mathematical model such as the exponential expression proposed by Schiff (1936)

Table 2. Calculated Count Rates Using All 4 Dead Time Expressions at a 1.5 μs Assumed Dead Time Constant where "1t" = Traditional Linear Expression, "2t" = Willis et al. (1993), "6t" = Six-Term Expansion, and "nt" = Logarithmic Expression. The "Observed" Count Rate is the Recorded Count Rate as it would be Measured in an Actual Instrument After Pulse Processing. The "Predicted" Count Rate is the Theoretical Count Rate as it would be upon Entering the Detector Before any Pulse Processing.

obsv cps	1t pred	1t obs/pre	2t pred	2t obs/pre	6t pred	6t obs/pre	nt pred	nt obs/pre
0	0	0	0	0	0	0	0	0
10,000	10,152.28	0.985	10,153.44	0.984888	10,153.46	0.984886	10,153.46	0.984886
20,000	20,618.56	0.97	20,628.13	0.96955	20,628.32	0.969541	20,628.32	0.969541
30,000	31,413.61	0.955	31,446.95	0.953988	31,447.99	0.953956	31,447.99	0.953956
40,000	42,553.19	0.94	42,634.83	0.9382	42,638.26	0.938125	42,638.26	0.938125
50,000	54,054.05	0.925	54,218.91	0.922188	54,227.67	0.922039	54,227.67	0.922039
60,000	65,934.06	0.91	66,228.82	0.90595	66,247.88	0.905689	66,247.88	0.905689
70,000	78,212.29	0.895	78,697	0.889,488	78,734.09	0.889069	78,734.09	0.889069
80,000	90,909.09	0.88	91,659.03	0.8728	91,725.59	0.872167	91,725.59	0.872167
90,000	104,046.2	0.865	105,154	0.855888	105,266.3	0.854974	105,266.3	0.854974
100,000	117,647.1	0.85	119,225	0.83875	119,405.6	0.837481	119,405.7	0.837481
110,000	131,736.5	0.835	133,919.7	0.821388	134,199.2	0.819677	134,199.3	0.819676
120,000	146,341.5	0.82	149,290.9	0.8038	149,709.9	0.80155	149,710.1	0.801549
130,000	161,490.7	0.805	165,397	0.785988	166,009.3	0.783089	166,009.7	0.783087
140,000	177,215.2	0.79	182,303.5	0.76795	183,178.8	0.764281	183,179.5	0.764278
150,000	193,548.4	0.775	200,083.4	0.749688	201,311.8	0.745113	201,313.2	0.745108
160,000	210,526.3	0.76	218,818.4	0.7312	220,515.8	0.725572	220,518.4	0.725563
170,000	228,187.9	0.745	238,600.7	0.712488	240,915.4	0.705642	240,919.8	0.705629
180,000	246,575.3	0.73	259,534.3	0.69355	262,655.3	0.685309	262,662.8	0.685289
190,000	265,734.3	0.715	281,737.1	0.674388	285,905	0.664556	285,917.5	0.664527
200,000	285,714.3	0.7	305,343.5	0.655	310,864.3	0.643368	310,884.8	0.643325
210,000	306,569.3	0.685	330,507	0.635388	337,770.3	0.621724	337,803.3	0.621664
220,000	328,358.2	0.67	357,404	0.61555	366,906.3	0.599608	366,958.8	0.599522
230,000	351,145	0.655	386,238.2	0.595488	398,614	0.576999	398,696.5	0.57688
240,000	375,000	0.64	417,246.2	0.5752	433,309.3	0.553877	433,437.6	0.553713
250,000	400,000	0.625	450,704.3	0.554687	471,503.4	0.530219	471,701.4	0.529996
260,000	426,229.5	0.61	486,937	0.53395	513,831.5	0.506002	514,135.1	0.505704
270,000	453,781.5	0.595	526,328.6	0.512988	561,093.4	0.481203	561,556.9	0.480806
280,000	482,758.6	0.58	569,337.1	0.4918	614,309.8	0.455796	615,015.9	0.455273
290,000	513,274.3	0.565	616,513	0.470388	674,804.8	0.429754	675,879.8	0.42907
300,000	545,454.6	0.55	668,523.7	0.44875	744,326.6	0.403049	745,966.3	0.402163

for extending dead times. Such an expression can be solved for I_{cps} by using the Lambert W-function which can be numerically evaluated. Unfortunately, this exponential expression is quite limited in practice, in that the product of the dead time and count rate cannot exceed $1/e$. This mathematically limits its application to count rates of 245 kcps or less at 1.5 μs and 123 kcps or less at dead times of 3 μs. Therefore, it is not considered further in this paper.

Discussion of the Various Dead Time Expressions

The predicted count rates from each of the four dead time correction expressions, i.e., traditional (Eq. (1)), Willis two-term (Eq. (2)), six-term expansion (Eq. (3)), and logarithmic (Eq. (4)) are shown in Table 2 to identify the mathematical (modeled) differences between the various expressions and can be examined graphically as shown in Figure 1, where we can see the dead time corrected theoretical (predicted) intensities for recorded (observed) intensities up to 300 kcps with a nominal dead time constant of 1.5 μs.

Note that the six-term expression plots underneath the logarithmic expression and is not visible in this plot, but which can be better resolved by plotting the observed count rate up to 400 kcps as seen in Figure 2. On an instrument with ~1.5 μs dead times (typical of JEOL instruments) and up to about 200 kcps, the traditional dead time expression appears to perform similarly. But above that count rate (or with higher dead time constants), the Willis et al. (1993) two-term expression begins to diverge, and above 200 kcps, the six-term or logarithmic expressions deviate even further. Though it must be noted that for quantitative analysis, the sensitivity of these graphical plots for predicted versus observed count rates is insufficient for properly evaluating these various expressions, as we will discuss further below.

For an instrument with roughly twice this dead time constant (typical of Cameca instruments), these corrections are even more significant. Assuming a dead time constant of ~3 μs, we obtain the following plot as seen in Figure 3 which, though limited to 200 kcps observed count rates, looks much the same as the 1.5 μs plot from Figure 2 which utilizes observed count rates to 400 kcps. In other words, the predicted count rates in Figure 3 are almost the same as Figure 2 yet with only half the input count rates. Hence, the typically higher dead time constants of Cameca instrument WDS spectrometers lose accuracy faster if not properly corrected, and the six-term and logarithmic expressions appear to start deviating from the traditional expression above ~100 kcps input count rates.

In addition, the gas detector itself can contain other latencies, for example, the time for the bias voltage to return to nominal while the gas ionization is neutralized. When the count rate increases to a time comparable to the duration of the gas ionization interval, the detector will undergo "paralyzing" behavior, and the observed count rate drops to zero. Though this gas ionization time constant appears to relatively insignificant until count rates over 500 to 1,000 kcps are

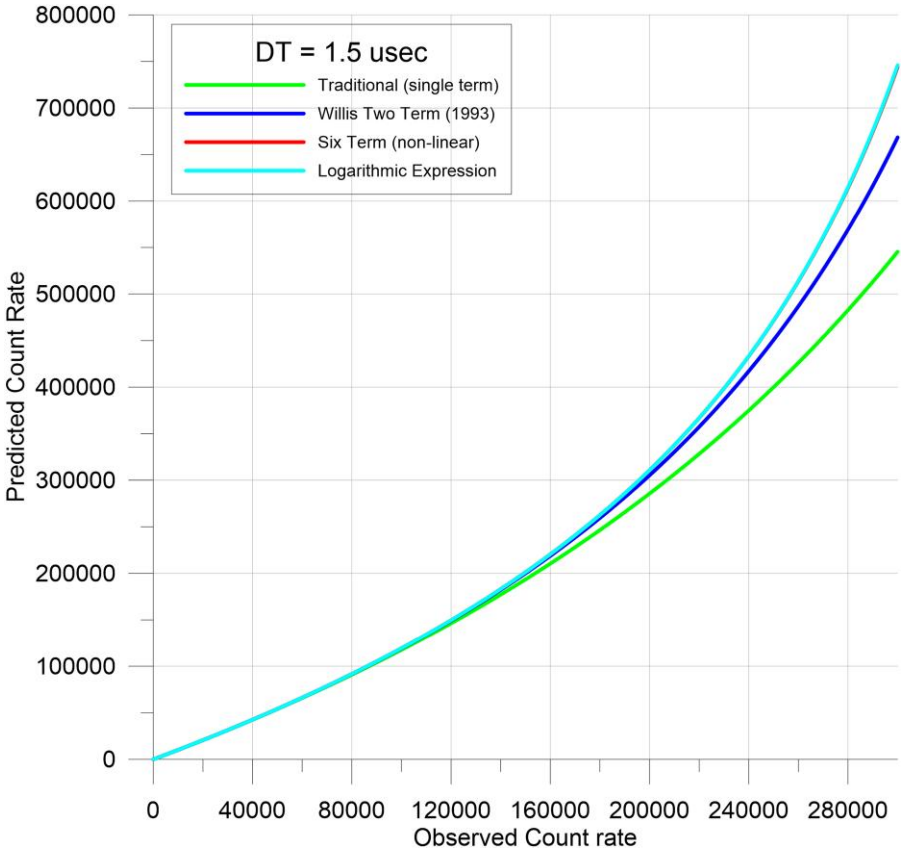

Fig. 1. Plotting all four dead time correction expressions at a dead time of 1.5 μs (typical for JEOL instruments), we can observe that all models converge towards zero and begin to diverge at observed count rates starting around 150 kcps. The six-term (red line) and logarithmic (cyan line) expressions are not distinguishable in this graphical plot.

attained (Beaman & Isasi, 1972; Bertin, 1975). In addition, possible decreases in intensity can occur due to satellite line production at very high beam currents which may be Bragg diffracted at an angle sufficient to be prevented from passing through the detector slit and therefore, uncounted (Rémond et al., 1996). All of these physics/hardware/electronics effects are generally included under the term "dead time", and could be modeled, but we will limit ourselves to modeling photon coincidence and the apparent nonlinear response of the pulse processing electronics, since these other effects generally occur at even higher counting rates than we are describing in this paper.

When the dead time becomes comparable to the actual time between photons, these curves approach an asymptote yielding untenably large dead time corrections, and the efficacy of all dead time expressions fails. As shown in Figure 4, at sufficiently high observed count rates and/or sufficiently high dead time constants, each of these mathematical expressions will fail eventually (when the evaluated polynomial term of dead time and count rate in the denominator of the various expressions exceeds 1). Still, even at more typical WDS dead time values, we are discussing theoretical (predicted) count rates exceeding 4,000 kcps for all these expressions, so our detectors/electronics will fail for other physical/hardware reasons long before such predicted count rates are actually generated and emitted from our interaction volumes.

Now some may question the need to calibrate our dead time constants at these high count rates, but from an instrumental calibration perspective, we should always prefer to measure a parameter under conditions that reveal its effects most clearly. Therefore, testing dead times at relatively low count rates (and therefore, with low precision) simply means that we are measuring our dead time constants at conditions where the effects are minimal and therefore, sub-optimal for determining the exact dead time constants with a high degree of accuracy.

Discussion of the Constant k-Ratio Method

With these improved dead time correction expressions in hand, we can now proceed to characterize the dead time constants on the WDS spectrometers themselves. Traditionally, we would simply plot our observed count rates versus our measured beam currents, and attempt to fit the slope of the observed count rates to the traditional linear dead time expression. But as we have discussed, such a calibration approach does not account for nonlinear response of the pulse processing system at moderate to high beam currents. In addition, such a procedure relies heavily on the linearity of the instrument's picoammeter, which may also be problematic.

We instead propose an apparently novel method for dead time calibration using simple k-ratios, which are the ratio of X-ray intensities of an element measured in two materials under the same conditions. The k-ratio is of course defined as

$$k = \frac{I_u}{I_s}. \quad (5)$$

where I_u is the secondary standard or unknown material and I_s is the primary standard, although any two materials

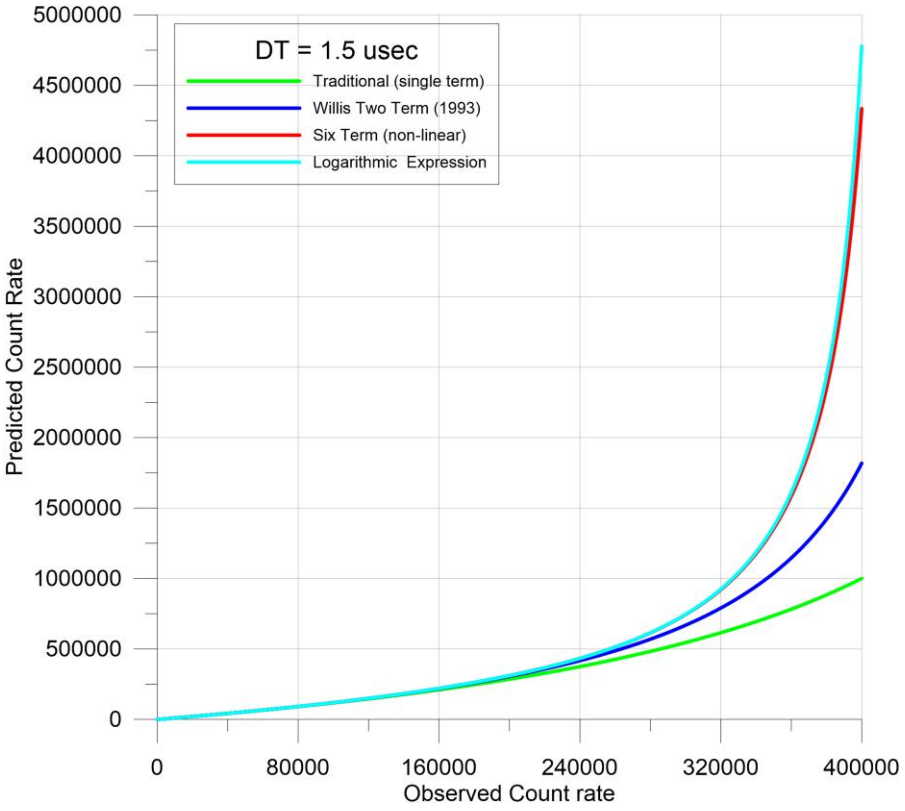

Fig. 2. Plotting all four dead time correction expressions again at 1.5 μs dead time but with an observed count rate up to 400 kcps. We can see a slight divergence of the logarithmic (cyan line) and six-term model (red line) predictions above 350 kcps.

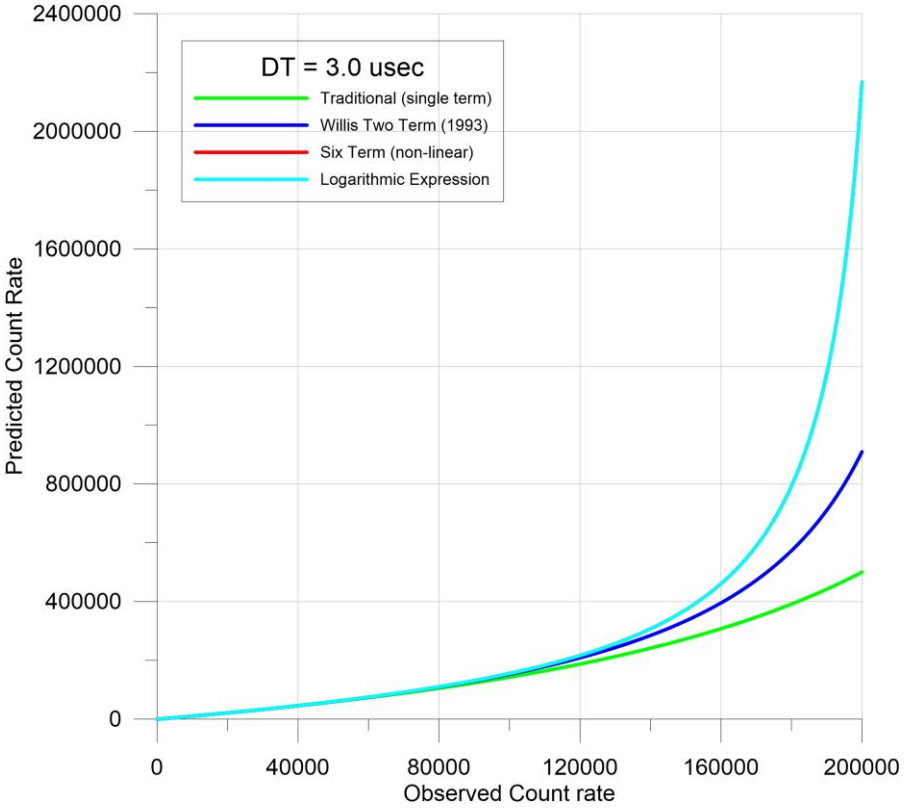

Fig. 3. Plotting all four dead time expressions with an assumed dead time of 3 μs (typical for Cameca instruments) but only up to 200 kcps observed count rates shows a very similar graph compared to Figure 1 with a dead time of 1.5 μs (typical for JEOL instruments), but with an even greater divergence. This is due to the Cameca instrument having an enforced dead time correction of roughly twice that of the JEOL instrument. Again, the six-term (red line) and logarithmic (cyan line) expressions are not distinguishable in this graphical plot up to 200 kcps.

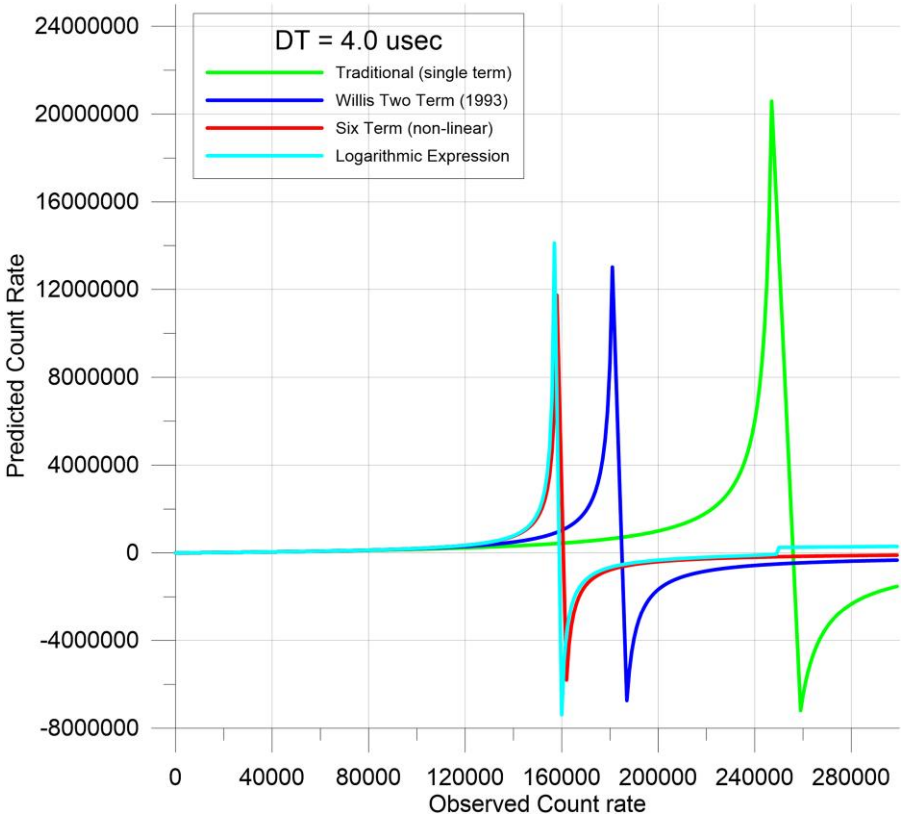

Fig. 4. By increasing the dead time constant to an arbitrarily high value (4 μs), we can see that mathematically all four dead time correction expressions ultimately fail spectacularly at high enough count rates. But, it should be noted that we are considering predicted count rates exceeding 10,000 kcps or more. Hardware pulse processing limitations will restrict our photon counting long before these levels are attained.

containing different concentrations of the element can be utilized.

We further make the simple (and in hindsight quite obvious) assumption that for a given emission line at a specific take-off angle and electron beam energy, we should obtain the same *k*-ratio at all beam currents for the two materials. For example, let us consider the observed count rates of two materials with significantly different concentrations of a given element utilized in the construction of a *k*-ratio, which produce significantly different intensities. This results in two observed intensities, each of which will require correction for dead time effects; the lower intensity requiring a smaller dead time correction, the higher intensity requiring a larger dead time correction. The difference in these two count rates then provides the algorithmic leverage necessary for us to very precisely calibrate the dead time constant. Using this constant *k*-ratio method, we then measure a number of *k*-ratios over a range of beam currents from low to high beam currents in order to properly stress the various dead time correction expressions.

Therefore, the constant *k*-ratio method is best performed using two materials with significantly different compositions. Typically, this means a primary standard containing the element of interest in high concentration (such as a pure metal or oxide) and a secondary standard that contains the element with a significantly lower concentration. To eliminate the effects of picoammeter nonlinearity during the dead time calibration procedure, we simply measure both the primary and secondary standards at the same beam current over a range of beam currents.

Because the measurement requires intensities from two materials (thus producing a *k*-ratio), it is somewhat related to the Heinrich ratio method (Heinrich et al., 1966) which utilizes two intensities from a single material, specifically the alpha and beta emissions of a pure metal such as copper. The advantage of the Heinrich method is that it also removes any picoammeter nonlinearity from the dead time calibrations because it utilizes the ratio of two intensities with significantly different count rates acquired at the same beam current (as is done with the constant *k*-ratio method proposed in this paper). The disadvantage of the Heinrich method is that it relies on an assumption of linear behavior in the detector and electronics, which as we will see breaks down at even moderate count rates and/or sufficiently large dead times.

The advantage of the constant *k*-ratio dead time calibration method over both the traditional calibration and the Heinrich ratio method is two-fold: (i) it is intuitive to utilize *k*-ratios as they are a fundamental metric that is universal to all EPMA measurements, and (ii) it has excellent sensitivity because as we regress the *k*-ratios to obtain a zero slope (horizontal fit) as a function of beam current or count rate, our *y*-axis can be expanded to reveal various subtleties in the *k*-ratio measurement data.

Typically, two materials are utilized to enable calibration of dead time constants on all WDS spectrometers simultaneously. For example, to measure Ti Kα *k*-ratios, one might use Ti metal and TiO_2 or $SrTiO_3$ for LIF (Lithium Fluoride) and PET (Pentaerythritol) Bragg crystals, and for Si Kα *k*-ratios, one might utilize SiO_2 (or even Si metal, because we do not care what the *k*-ratio actually is, only that it remains constant

over a range of beam currents) and a synthetic silicate such as Mg_2SiO_4 or other silicate mineral for PET and TAP (Thallium Acid Phthalate) Bragg crystals. Obviously, these materials should be resistant to beam damage at high currents, though the electron beam can be defocused to minimize sample damage and/or charging effects. Note that the two materials utilized must also be homogeneous, though their exact compositions are not important (in fact, they can even be of unknown composition), merely that they are significantly different in their concentrations and therefore, their respective count rates.

Once the appropriate materials have been identified, the next step is to acquire multiple datasets of the primary and secondary standards over a range of beam currents starting at low beam currents of 5 to 10 nA in order to obtain the "nominal" *k*-ratio, that is, a *k*-ratio with minimal dead time effects. As the beam current is progressively increased and both primary and secondary materials are re-measured at each beam current, the *k*-ratio of the secondary standard relative to the primary standard should remain constant within counting precision and the stability of the instrument. But since the count rates of the primary and secondary standards are significantly different, the *k*-ratio produced will be very sensitive to the dead time correction expressions and the dead time constants utilized.

Specifically, if the *k*-ratios measured over a range of beam currents exhibit a positive slope trend with increasing beam current, the dead time constant is probably too low (the primary standard intensity in the *k*-ratio denominator is decreasing faster than the numerator with increasing beam current), and the dead time constant should be increased. Alternatively, if the dead time constant is too large, the range of *k*-ratios should show a negative slope (the primary standard intensity in the *k*-ratio denominator is increasing faster than the numerator with increasing beam current).

The degree of slope in the *k*-ratios that one decides is tolerable depends on the accuracy of the dead time calibration desired, however, the resulting quantitative accuracy is easily estimated by comparing these *k*-ratios measured at different beam currents. Again, it is worth noting that beam stability is less important with the constant *k*-ratio method since we are measuring both the primary and secondary materials at the same beam current. Beam current drift is usually expected to be minimal over a few minutes on a well aligned column with an appropriately adjusted emission source, though both measured intensities in the *k*-ratio can also be normalized for beam current drift as one typically does since we are merely constructing *k*-ratios as we normally would in quantitative microanalysis.

Using this method, we have found that we are able to perform quantitative measurements at beam currents of ~200 nA or more, which on Ti metal and a large area PET crystal can yield input count rates of up to 300 to 400 kcps! In addition, the constant *k*-ratio method allows for a number of other instrumental calibrations, all utilizing the same dataset. Specifically, the constant *k*-ratio dataset can be utilized for three separate calibration checks on EPMA instruments:

1. Calibration of dead time constants on each spectrometer by measuring *k*-ratios using multiple beam currents on primary standards and secondary standards. That is to say, these *k*-ratios, measured on each spectrometer at a number of different beam currents, should all be the same (within statistics) if the dead time constant for that spectrometer is correct (and an appropriate nonlinear dead time expression is utilized). This is independent of the picoammeter calibrations because both materials are measured at the same beam current, though the zero-regression slope depends slightly on the dead time correction expression utilized as expected.
2. Checking the picoammeter accuracy/linearity by utilizing the same *k*-ratio data, but this time instead of using primary and secondary standards acquired at the same beam current, we calculate the *k*-ratios using a single primary standard (acquired at a single beam current) and plotting the *k*-ratios of the secondary standards (acquired over a range of beam currents) to check that they are still consistent as a function of beam current. This test will reveal problems with the picoammeter linearity since one is extrapolating from a single beam current to other beam currents.
3. Using this same constant *k*-ratio dataset, by plotting the *k*-ratios of all the spectrometers using the same element and emission line, we obtain a "simultaneous *k*-ratio" test that compares the *k*-ratios from all spectrometers to see how well they agree with each other. Disagreement of the *k*-ratios between the various spectrometers may indicate a spectrometer alignment and/or asymmetrical Bragg diffraction (and/or specimen tilt) issue resulting in small but critical differences in the effective take-off angle of each spectrometer.

Interestingly, because these *k*-ratio datasets can be acquired just as we would with typical quantitative sample acquisitions, secondary measurement effects such as differences in coating thickness/materials and/or beam damage effects can be corrected for quite easily. Though again, it should be noted that the actual *k*-ratio obtained is not important, only that these *k*-ratios remain constant as a function of beam current/count rate.

Sensitivity of the Constant k-Ratio Method

At low to moderate count rates typically utilized in WDS microanalysis, the effects of nonideal pulse shapes on our dead time models are more difficult to determine, hence, the need to increase the range of count rates which are utilized to determine these nonlinear dead time effects.

Aside from being immune to problems of picoammeter linearity, the constant *k*-ratio has a significant advantage over other methods in sensitivity for estimation of the dead time constant (and picoammeter or simultaneous *k*-ratio tests that we choose to perform), and that is simply due to the fact that we are testing for a regression slope of zero in our *k*-ratios (hence, the term "constant" *k*-ratios). In other methods (Ruark and Brammer 1937, Heinrich et al., 1966) by regression of the trend for a nonzero slope, we are unable to expand the *y*-axis to examine the data with enough sensitivity. With the constant *k*-ratio method on the other hand, because it seeks a constant *k*-ratio over a wide range of count rates/beam currents, one can easily expand the *y*-axis to discern very subtle differences in the data.

Note that when examining constant *k*-ratio data at this level of sensitivity (down to a few hundred ppm when quantified in some cases), we can discern many different effects that each

contribute towards a general dead time correction, which might include, simple photon coincidence, pulse processing electronics, paralyzing behavior due to gas ionization, spectrometer and instrumental misalignment, and even satellite peak production at very high count rates.

We do not claim that these new dead time expressions correct for all of these nonlinear effects in the X-ray detection system. However, the constant *k*-ratio method can certainly be utilized to further tease out these other counting artifacts at even higher count rates, all of which fall under the general term of the dead time correction.

Discussion of Experimental Results

Data was acquired on the JEOL iHP200F instrument at the University of British Columbia and the Cameca SX100 at the University of Oregon. In Figure 5a, we can see the *k*-ratios from the JEOL iHP200F using Ti metal as a primary standard and TiO_2 as a secondary standard, plotted using the traditional dead time expression with a dead time constant determined by JEOL at relatively low count rates where photon coincidence is the dominant feature. At even moderate count rates (>~50 kcps), the traditional linear expression clearly fails to produce consistent Ti Kα *k*-ratios from TiO_2/Ti. In Figure 5b, we see an attempt to correct these higher count rates by arbitrarily increasing the dead time constant from 1.32 to 1.6 μs, but that effort merely over corrects low count rates while still under correcting higher count rates. However, in Figure 6, we can see that the two-term Willis et al. (1993) expression produces constant *k*-ratios up to ~150 kcps or so using our original dead time constant of 1.32 μs, which by itself is a worthy improvement in quantitative accuracy. Plotting up the same data in Figure 7 using the newly derived logarithmic expression Eq. (4), we can see that although there is a further improvement in consistency of the *k*-ratios, we can see that we have slightly over-corrected our *k*-ratio intensities because we now need to make a small adjustment in the dead time (parametric) constant as described previously. Note that the predicted intensities from the logarithmic expression are essentially identical to the values predicted by six-term Maclaurin series expression Eq. (3).

Because the traditional dead time expression underestimates the nonlinear dead time effects of the pulse processing electronics at even moderate count rates, dead time constants obtained using that expression tend to overestimate the actual dead time constants compared to using the expanded dead time expressions discussed in this paper, as seen in Table 3. Hence, the estimated dead time constant from the traditional linear regression biases the actual dead time constant slightly higher than it should be. By using the logarithmic expression and adjusting the dead time constant down slightly from 1.32 μs to 1.29 μs to account for these nonlinear pulse shape effects properly, we obtain the plot shown in Figure 8 which exhibits constant *k*-ratios very close to the zero slope we are seeking. Depending on the accuracy requirements of the laboratory, the range over which the *k*-ratios remains constant can be evaluated quantitatively by converting the *k*-ratios obtained into concentrations.

To compare the various dead time models more clearly, we can combine these last few figures as seen in Figure 9 which demonstrates how the constant *k*-ratio method allows us to evaluate these various expressions with high sensitivity when plotted as *k*-ratios from TiO_2/Ti as a function of beam currents ranging from 10 to 140 nA (~28 kcps to ~390 kcps as measured on Ti metal primary standard). Note particularly how all methods yield the similar results (within statistics) at low count rates as expected. At even lower count rates, all

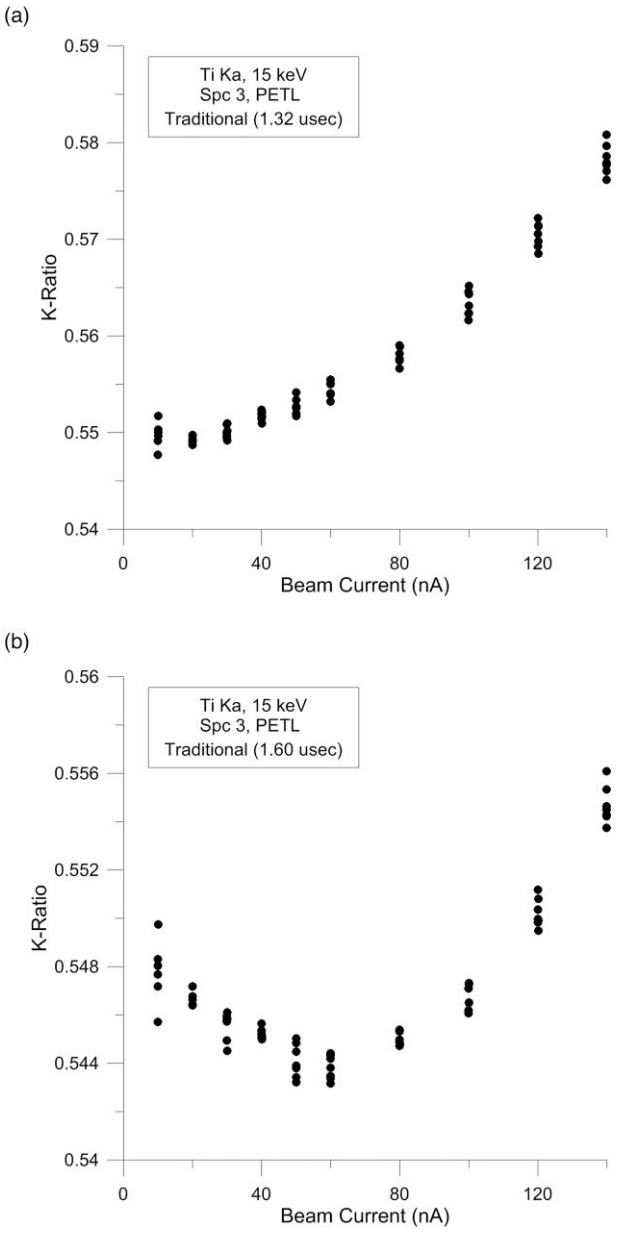

Fig. 5. Ti Kα *k*-ratios from TiO_2/Ti metal from 10 nA (~28 kcps) to 140 nA (~400 kcps) on a PETL Bragg crystal at 15 keV plotted using the traditional linear dead time expression. Depending on the value of the dead time constant, the measured *k*-ratios either increase or decrease with beam current because the Ti metal intensities in the denominator of each *k*-ratio are affected more than the TiO_2 secondary standard intensities (due to the difference in concentrations of Ti). Therefore, dead time effects are observed more severely in the Ti metal primary standard intensities than in the TiO_2 secondary standard intensities providing the algorithmic leverage for determining the correct dead time constant using the "constant *k*-ratio" method. Utilizing the traditional dead time correction expression with a dead time constant of 1.32 μs using JEOL's own linear calibration (**a**) works well at count rates under 30 nA (~80 kcps) but starts to fail at higher count rates. Until now, analysts have had to limit themselves to such low to moderate count rates for quantitative analysis. Attempting to correct high count rates using the traditional dead time expression by arbitrarily increasing the dead time constant (**b**) causes low count rates to be over corrected and higher count rates to still be under corrected, demonstrating the nonlinear response of the counting system which must therefore be corrected using a nonlinear approach.

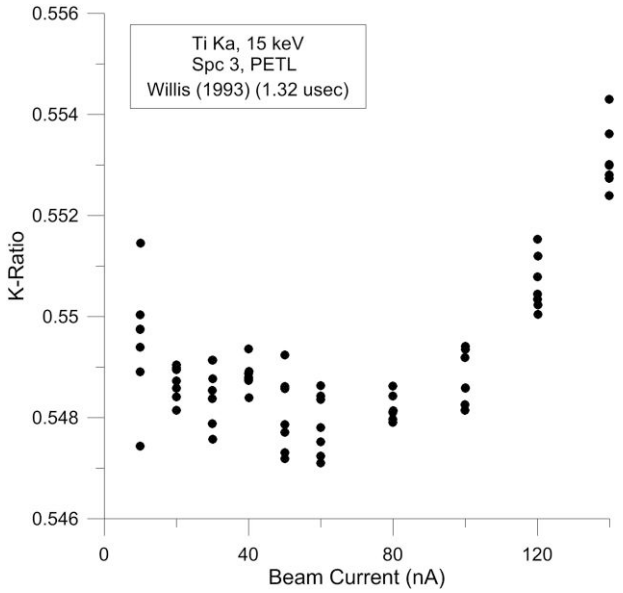

Fig. 6. Plotting the same Ti Kα *k*-ratio data from Figures 5a and 5b, the Willis et al. (1993) two-term dead time expression properly corrects the data at low to moderate count rates, but still fails at count rates over ~200 kcps (~280 kcps on Ti metal at 100 nA). However, note the much reduced range in the *y*-axis compared to Figure 5 demonstrating improved accuracy at higher count rates.

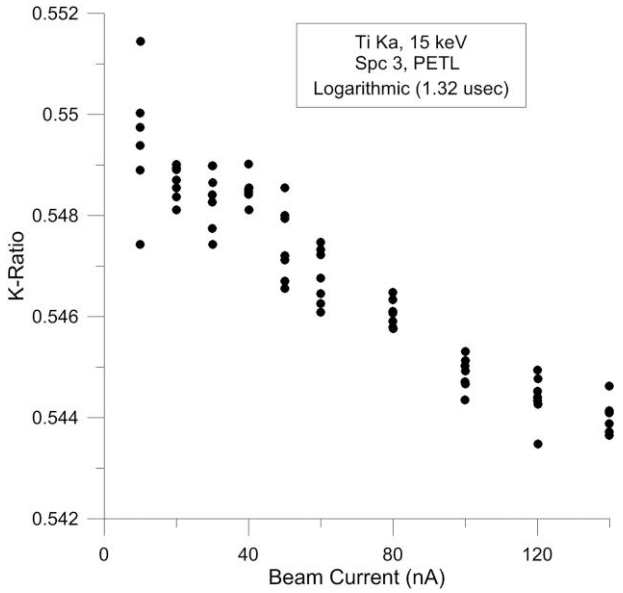

Fig. 7. Again, plotting the Ti Kα *k*-ratio data from Figures 5 and 6, the logarithmic expression slightly over corrects the Ti Kα *k*-ratios at high count rates when using a dead time constant originally calibrated using the traditional linear fit method. Due to nonlinear effects of the detector and pulse processing electronics at high count rates, the traditional expression produces dead time constants which are slightly biased towards higher values when utilizing count rates over ~50 kcps. In fact, the dead time constant is a "parametric" constant since its exact value depends on the form of the dead time expression utilized to measure it.

expressions converge towards identical results. In fact, at 1.5 μs dead times, the traditional and logarithmic expressions produce results that are the same within one part in 10,000,000 at 1,000 cps, one part in 100,000 at 10 kcps, and one part in 10,000 at 20 kcps.

Table 3. Optimized Ti Kα Dead Times on Ti Metal and TiO_2, UBC JEOL iHP200F, Comparing Dead Time Constants Obtained by JEOL using the Traditional Linear Method and also using the Constant *k*-Ratio Method with the Logarithmic Expression. On all Spectrometers, the Logarithmic Method Produces a Lower Dead Time Constant as Expected. Hence, the use of the Term "Parametric" Constant for these Dead Time Intervals.

Sp1	Sp2	Sp3	Sp4	Sp5	
PETJ	LIFL	PETL	TAPL	LIFL	
1.52	1.36	1.32	1.69	1.36	(μs) using traditional method
1.26	1.26	1.29	1.1	1.25	(μs) using logarithmic method

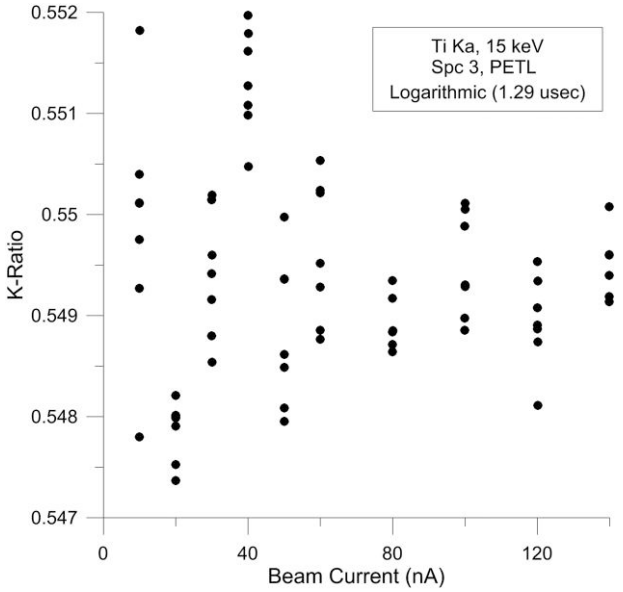

Fig. 8. Ti Kα *k*-ratios corrected using the logarithmic dead time expression where the dead time (parametric) constant was adjusted slightly, from 1.32 μs to 1.29 μs. We now obtain a relatively constant *k*-ratio (within statistics) over a wide range of count rates/beam currents suitable for quantitative analysis even at count rates up to ~400 kcps. The sensitivity of the constant *k*-ratio method is quite apparent in this figure by noting the relatively small range of *k*-ratios displayed on the *y*-axis.

Picoammeter Calibration

Once our dead time constants are properly calibrated on each spectrometer, we can also test our instrument picoammeter linearity. This is important as X-ray counts are typically normalized to the measured beam current, especially when using multiple beam current in an analysis, for example, when measuring primary standards at 30 nA and trace elements at 200 nA. Figure 10 reveals that we can ascertain the accuracy of our picoammeter using the same constant *k*-ratio dataset by simply utilizing a single primary standard measured at a single beam current and plotting the *k*-ratios for all secondary standards measured at multiple beam currents. If the picoammeter response is linear, we should see a flat line response (constant *k*-ratio) at all beam currents using a single primary standard and extrapolating to the other secondary standards which are measured over a range of beam currents. In Figure 10a, we see results from a Cameca SX100 where the picoammeter exhibits excessive nonlinearity particularly in the

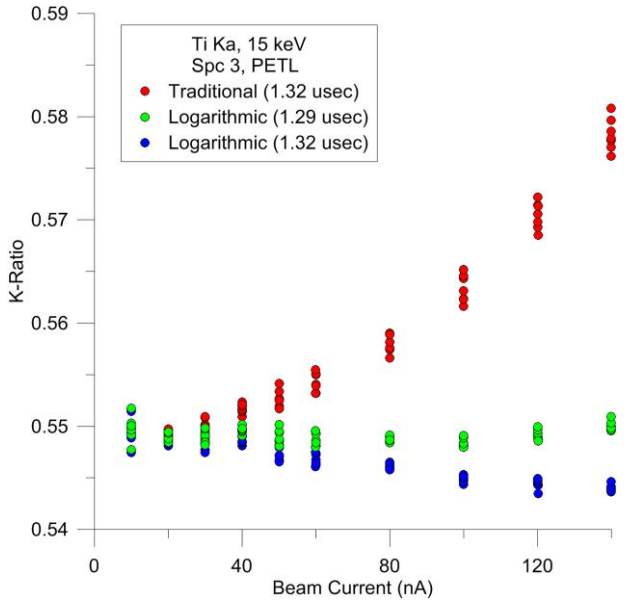

Fig. 9. Combined plot of *k*-ratios versus beam current showing the traditional dead time expression using the dead time constant obtained from the traditional calibration of dead time (per JEOL engineer) of 1.32 μs (red symbols), the same data plotted using the logarithmic expression also using a dead time constant of 1.32 μs (blue symbols), and the same data plotted using the logarithmic expression using a dead time constant of 1.29 μs (green symbols) which was adjusted to yield a zero slope regression over a large range of beam currents (count rates from ~28 kcps to ~400 kcps).

transition from the 5 to 50 nA picoammeter range to the 50 to 500 nA picoammeter range. In Figure 10b, the JEOL iHP200F picoammeter shows excellent linearity over a similar range of beam currents.

Simultaneous k*-Ratio Comparisons Using Multiple Spectrometers*

The excellent sensitivity of the constant *k*-ratio method means that we can also utilize the same constant *k*-ratio dataset (if we measured *k*-ratios on more than one WDS spectrometer) to assess our instrumental consistency by comparing *k*-ratios from multiple spectrometers (Fig. 11), as they should all agree within statistics if our instrument is properly calibrated and aligned. Also note that at count rates over 400 kcps, we begin to observe other perhaps "paralyzing" behaviors of the gas detector and/or possibly satellite line production, as seen for spectrometer 3 (PETL) as both effects would primarily decrease the count rates of the primary standard, hence, resulting in small increases in the *k*-ratio values at these highest count rates (Goldstein et al., 1992, p363).

It should also be noted that we must ask ourselves: how can we begin to compare our *k*-ratios from one instrument to another if we cannot even obtain consistent *k*-ratios from all of the spectrometers on our own instrument?

Possible reasons for observing these systematic differences between various spectrometers on a single instrument are beyond the scope of this paper, but we can point to several lines of investigation that might be pursued, as all are in effect the result of small differences in the *effective* take-off angle of the spectrometer. First of all, a spectrometer mechanical mis-alignment can produce differences in the effective take-off angle from the other spectrometers.

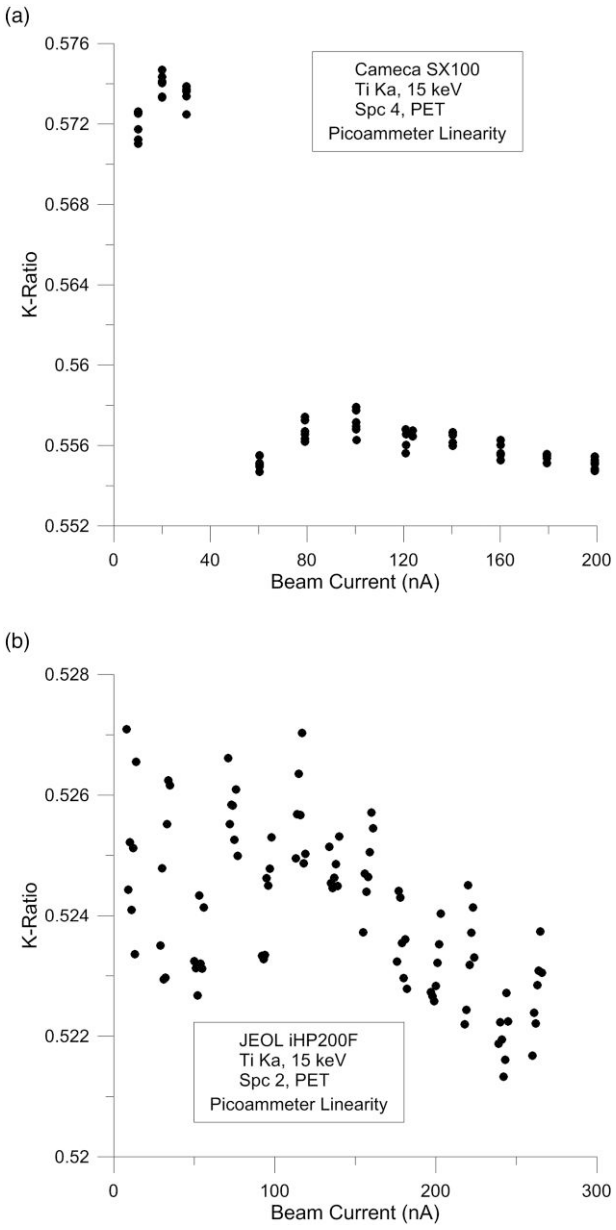

Fig. 10. By plotting our secondary (TiO_2) standard *k*-ratios measured at multiple beam currents, against a single primary standard (Ti metal) measured at a single beam current (10 nA), we can test the linearity of our picoammeter over a range of beam currents by extrapolating from our primary standard. In **a**, the Cameca SX100 instrument picoammeter linearity is plotted from 10 to 200 nA showing excessive nonlinearity at the 50 nA "crossover" threshold region, thus requiring adjustment of the picoammeter circuits using a calibrated current source. In **b**, the JEOL iHP200F instrument picoammeter linearity is also plotted from 10 to 200 nA showing relatively low levels of nonlinearity over the entire range of beam current.

Additionally, *asymmetrical* diffraction of the Bragg crystals can also produce different effective take-off angles relative to the column and specimen plane. Even more concerning is the alignment of the column relative to the spectrometers. In other words, is the electron column centered relative to all the spectrometers and their Rowland circles? All of these effects including specimen tilt can contribute to differences in effective take-off angles for each spectrometer and therefore, produce differences in the *k*-ratios measured on different spectrometers.

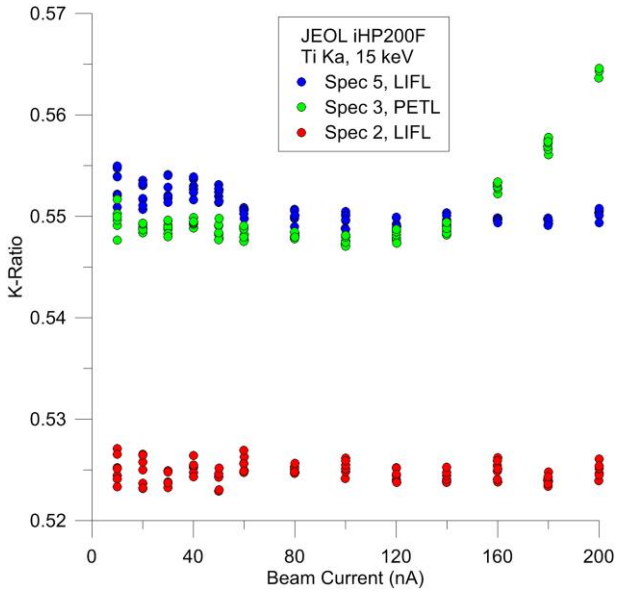

Fig. 11. By plotting Ti Kα *k*-ratios from multiple spectrometers, we can obtain high sensitivity comparisons between our various WDS spectrometers (and EDS if desired). Here, we can see *k*-ratios from spectrometer 5 (LLIF) (blue symbols), which produces a significantly Ti Kα lower count rate (~100 kcps at 100 nA), does not demonstrate so called "paralyzing" behavior seen in the much higher count rate spectrometer 3 (PETL) (green symbols) at count rate above 400 kcps (at 140 nA of beam current). This "paralyzing" behavior could also be due to a number of causes other than photon coincidence, including limits to electronic multiplexing in the pulse processing circuitry, increased production of doubly ionized atoms (satellite emissions) at high beam currents which could "steal" photons from the main emission line for high spectral resolution WDS spectrometers or it could be due to constant ionization of the detector gas. But, we can also observe that spectrometer 2 (LIFL) (red symbols) is producing consistently lower *k*-ratios than the other two spectrometers. Possible explanations include sample tilt, spectrometer alignment, asymmetrical diffraction of Bragg diffractors, and mechanical offset of the spectrometers from the electron column. These consistent differences in the observed *k*-ratios from a spectrometer result from slightly different "effective" take-off angles for each spectrometer/Bragg crystal combinations requiring either spectrometer re-alignment or Bragg crystal replacement. Alternatively, we might model these differences in the absorption correction path length using optimized effective take-off angles for each spectrometer/Bragg crystal combination.

There is hope however that once these "effective" take-off angles for each spectrometer (and Bragg crystal) are characterized and found to be consistent, it should be possible to utilize an experimentally measured effective take-off angle for each spectrometer on our instruments as opposed to simply assuming the nominal take off angle of 40 degrees. This calibrated effective take off angle for each spectrometer can then be utilized in the absorption correction in the matrix correction to further improve quantitative analysis accuracy. Whatever the reasons, when we obtain systematically different *k*-ratios on our instruments, we now have an excellent dataset to pursue further instrument calibrations, including inter-laboratory comparisons of instrumental and standard *k*-ratio consensus.

Performing Constant k-Ratio Calibrations on Your Instrument

The first step in the constant *k*-ratio method is to acquire an appropriate set of *k*-ratios. Typically, one would use two materials with significantly different concentrations of an element, though the specific element and emission line are totally optional. Also, the precise compositions of these materials are not important, merely that they are homogeneous (and beam stable). All we are looking for is a *constant k*-ratio as a function of beam current/count rate.

In general, we seek a pair of materials such that the k-ratio obtained on the secondary standard is approximately between 0.2 and 0.6. If the *k*-ratio is too small, the measurement precision will be decreased, and it will be more difficult to precisely characterize these dead time effects. If the *k*-ratio is too large, the difference in the two count rates will be small, and the dead time expression will not be sufficiently stressed and therefore, less sensitive to dead time effects.

We suggest starting with Ti metal and TiO_2 as suggested before because they are both beam stable, easy to obtain, and can be used with both LIF and PET crystals. We further suggest measuring Ti Kα on all spectrometers possible, so that each spectrometer can be calibrated for dead time. One can also use two Si bearing materials, e.g., SiO_2 (or even Si metal) and Mg_2SiO_4 for TAP and PET crystals, though in all cases, the beam should be defocused to 10 to 15 μm to avoid beam damage and/or charging effects.

Additionally, the adjustment of the PHA settings for each spectrometer is absolutely critical for accurate *k*-ratio measurements over such a large range of count rates, in order to avoid pulse height depression effects as demonstrated in Figure 12. Specifically, one must be sure to keep the PHA peak within the pulse processing range of our electronics. That generally means keeping the PHA peak from dropping below the baseline voltage due to pulse height depression at the highest count rates. We find that adjusting the PHA settings at the highest beam current utilized while on the primary standard (with the highest concentration), and adjusting the gain (for Cameca instruments) or the bias (for JEOL instruments) to ensure that the PHA peak (and escape peak if present) are kept above the baseline level, even though some pulses appear to be "cutoff" by the maximum PHA voltage displayed in Figure 13. At lower beam currents and/or lower concentrations (lower count rates), the PHA peak will shift to the right, but in fact, all pulses will still be counted properly in "integral" PHA mode, so long as the PHA peaks at the highest count rates are above the baseline level.

Therefore, it is recommended to perform all these constant *k*-ratio measurements in "integral" PHA mode, not "differential" mode. At lower count rates, the PHA peak will shift to higher voltages, and even beyond the range of our displayed PHA distributions, but if the PHA is in "integral" mode, this PHA peak shifting will (surprisingly enough) not affect the observed count rates and therefore, not affect the *k*-ratio intensity measurements.

Start the constant *k*-ratio acquisitions by measuring both the Ti metal and TiO_2 at 5 or 10 nA (after checking for suitable background positions). For sufficient precision, one might need to count for 60 or more seconds on peak, especially at these lower beam currents. This can be done at whatever beam voltage one prefers (15 or 20 kV works fine, though the higher the voltage, the higher the count rate and the smaller the surface effects which has statistical benefits) for ascertaining measurement statistics. Then, measure 5 to 10 points for our *k*-ratios at each chosen beam current up to 100 to 200 nA or even more, for example, 5, 10, 20, 40, 60, 80, 100, 120, 140, 160, 180, and 200 nA. Although, Cameca instruments might want to avoid measurements between 40 and 50 nA due to the design of the Cameca column and depending how well aligned it is.

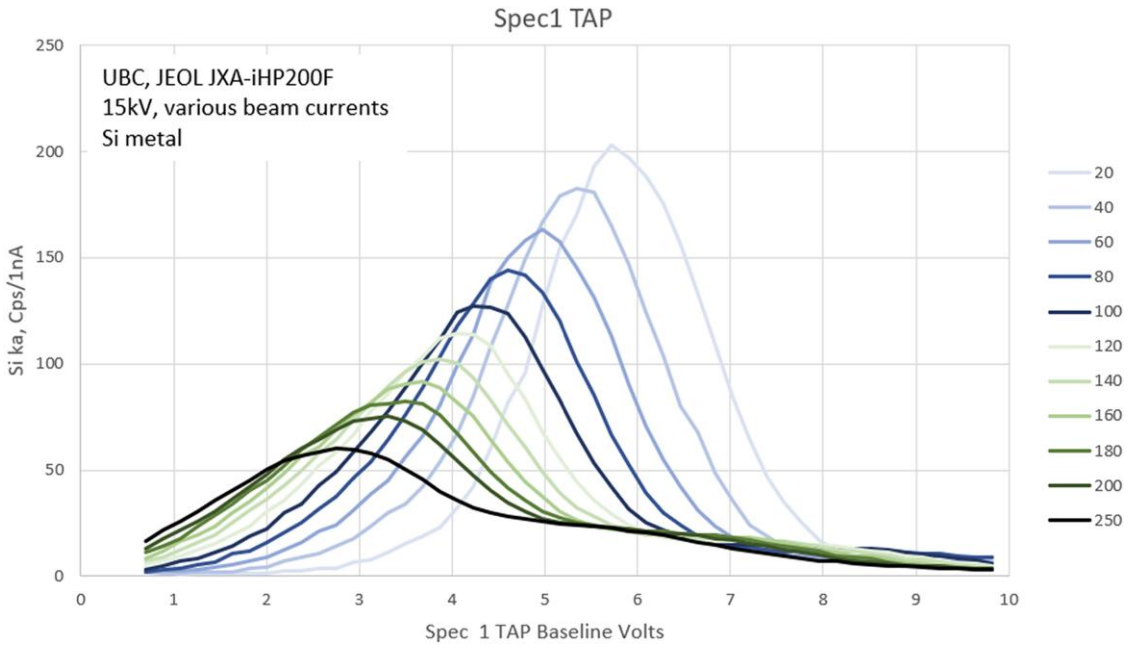

Fig. 12. PHA distributions for Si Kα measured in Si metal at 15 keV over a range of beam currents from 20 to 250 nA. Note the progressive shift of the PHA peak to lower voltages due to pulse height depression as the beam current is increased. Due to this pulse height depression at high count rates, the PHA gain and/or bias should always be adjusted at the highest expected beam current using a material with the highest expected concentration of the element. This ensures that the full PHA distribution remains above the baseline level of the PHA electronics and avoids a nonlinear response of the spectrometer over the full range of count rates.

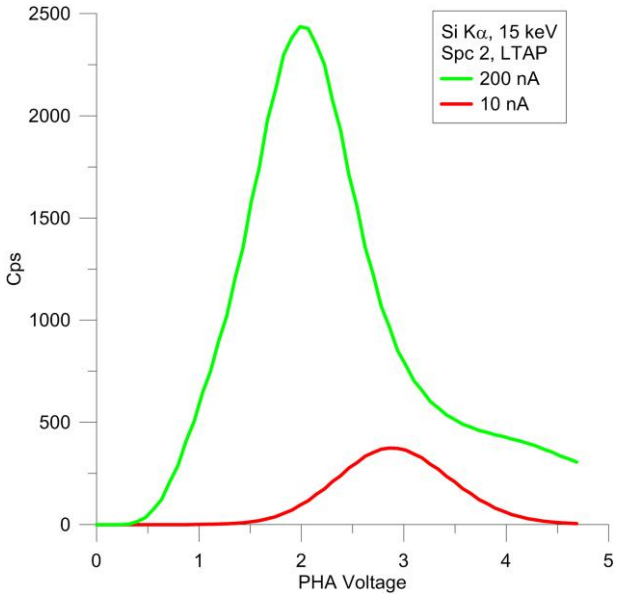

Fig. 13. Properly adjusted PHA settings allow quantitative analysis over a large range of beam currents (proxy for count rates). It is critical to adjust ones PHA settings to ensure that at the highest count rates expected to be encountered (highest expected beam current and highest expected concentration), the PHA peak is completely above the baseline setting. Although the PHA scan at 200 nA appears to be cutoff above ~4.7 V, surprisingly in "integral" PHA mode, all pulses above the baseline level are still integrated for quantitative analysis, as determined by measurements of intensities over range of gain/bias settings on both Cameca and JEOL instruments.

It is important that one must be sure to measure these *k*-ratio materials in pairs at each beam current so that any potential picoammeter inaccuracy will be zeroed out. In fact, this is one of the main advantages of this constant *k*-ratio dead time calibration method over the traditional method which depends on the accuracy of the picoammeter. Therefore, in order to ensure that the *k*-ratios are constructed using a primary standard and a secondary standard both measured using the same beam current, always acquire each primary standard before each secondary standard and turn off any standard intensity drift corrections if your software utilizes this feature.

The *k*-ratios measured at the lowest beam currents (proxy for count rates) will have very small dead time corrections as the count rates are relatively low, and for that reason, we can therefore assume that these *k*-ratios are also the most accurate with regard to the dead time correction. It is our goal to adjust our dead time constants for each spectrometer until the *k*-ratios obtained at higher beam currents (count rates) yield the same *k*-ratios (within statistics) as the *k*-ratio measurements at the lowest beam currents.

Then, simply plot the secondary standard *k*-ratios as a function of beam current, from intensities corrected using a nonlinear dead time expression (such as the logarithmic equation). Next, observe the slope trend of the *k*-ratios, while adjusting the dead time constant to produce a zero slope trend. The default dead time constants in some analysis software can then be edited based on these more accurate values and utilized in subsequent quantitative point analyses and quantitative mapping to produce more quantitative results at low, moderate, and high beam currents.

Some other items to note: there is some controversy over whether dead time varies as a function of X-ray emission energy and/or PHA gain or bias. However preliminary measurements by some of us show no consistent trends in the optimized dead time constants. What about satellite line production? Ostensibly, satellite line production should be favored at high electron fluxes, and this effect would shift photons emitted at the primary emission peak, to a secondary

(satellite) emission peak, resulting in a loss of the primary intensity in turn causing an increase in our *k*-ratios. More data is necessary to test these additional hypotheses.

It should also be noted that all these dead time effects could be greatly reduced for both JEOL and Cameca instruments through the development of better/faster electronics. Current instruments sadly rely on electronic pulse processing technology dating from the 1980s and 1990s and could be improved significantly with modern field programmable gate array electronic circuit designs (Abbene et al., 2013).

Conclusions

We demonstrate that the traditional dead time correction model does not properly account for the nonlinear behavior of the photon pulse processing electronics in WDS spectrometers at moderate to high count rates. By including additional terms of this Maclaurin like expansion series, it is possible to improve dead time modeling for count rates up to ~400 kcps, thereby improving accurate quantification across a wide range in X-ray count rates (and concentrations). By integrating all these terms into a logarithmic expression, we can fully account for not only photon coincidence but also the nonlinear response of the pulse processing system up to the current limits of our WDS hardware and electronics.

We propose a new method for calibration of dead time constants utilizing the method of constant *k*-ratios. This approach offers the advantage of nullifying any possible picoammeter nonlinearities since both the primary and secondary standards in each *k*-ratio are measured at the same beam current. This method provides an easy and intuitive method to adjust dead time constants to yield a zero slope fit of our *k*-ratios. And because of the high sensitivity of this method, we can obtain accurate determinations of our dead time constants for quantitative analysis at count rates up to several hundred kcps or more.

Furthermore, the same constant *k*-ratio dataset can also be utilized to provide high sensitivity evaluations of our picoammeter linearity, by applying a single primary standard intensity to all the *k*-ratios measured at different beam currents. The importance of a properly calibrated picoammeter can be imagined by considering the analysis of major elements at one beam current and minor or trace element at a different beam current. If the picoammeter is found to be nonlinear, the use of a constant current source may be required to properly calibrate the picoammeter electronics.

In addition, this same dataset (from multiple spectrometers) also allows us to evaluate our "simultaneous" *k*-ratios to ensure that the effective take-off angle of each of our spectrometers (including our EDS detectors) is in agreement with each other. With respect to comparing (consensus) *k*-ratio results from one laboratory with another, we obviously should be sure that our instrument is in good agreement with itself, before making any such inter-laboratory comparisons!

In summary, we present a new method for calibration of dead time constants, picoammeter calibration, and simultaneous *k*-ratio testing of multiple spectrometers with the acquisition of a single *k*-ratio dataset. In addition, we present a new logarithmic dead time correction expression which is applicable over a wide range of count rates, typically 8 to 10 times greater than typically utilized with the traditional linear dead time expression. The benefits of this new logarithmic dead time model for quantitative analysis are the ability to analyze major and minor elements at high beam currents simultaneously with trace element sensitivity and also the ability to perform high speed quantitative mapping at high beam currents where the measured elements are present in various phases as major, minor or trace element concentrations.

Acknowledgments

The authors would like to acknowledge Edward Vicenzi (The Smithsonian Institution) as an internal reviewer for this manuscript. His comments and suggestions were most helpful. We would also like to thank Petras Jokubauskas (University of Warsaw) for many enlightening discussions on the details of dead time effects and pulse processing of WDS electronic systems.

Financial Support

The current study has not received any funding from any organizations or institutions.

Conflict of Interest

John Donovan is the president of Probe Software which offers automation and analysis software for EPMA instruments.

References

Abbene L, Gerardi G & Principato F (2013). Real time digital pulse processing for X-ray and gamma ray semiconductor detectors. *Nucl Instrum Methods Phys Res* **730**, 124–128. https://doi.org/10.1016/j.nima.2013.04.053

Beaman DR & Isasi JA (1972). *"Electron Beam Microanalysis."* Philadelphia: American society for testing and materials.

Beaman DR & Solosky LF (1972). Accuracy of quantitative electron probe microanalysis with energy dispersive spectrometers. *Anal Chem* **44**(9), 1598–1610. https://doi.org/10.1021/ac60317a009

Bertin EP (1975). X-ray secondary-emission (fluorescence) spectrometry; General introduction. *Principles Pract X-Ray Spectromet Anal*, 89–112.

Donovan JJ, *et al.* (2021). Quantitative WDS compositional mapping using the electron microprobe. *Am Mineral: J Earth Planetary Mater* **106**(11), 1717–1735. https://doi.org/10.2138/am-2021-7739

Geller JD & Herrington C (2002). High count rate electron probe microanalysis. *J Res Natl Inst Stan Technol* **107**(6), 503. https://doi.org/10.6028/jres.107.043

Goldstein JI, *et al.* (1992). *Scanning Electron Microscopy and X-Ray Microanalysis. A Text for Biologists, Materials Scientists, and Geologists*. xviii+–820 pp. New York, London: Plenum Press.

Heinrich KFJ, Vieth D, & H Yakowitz. (1966) *"Correction for Non-Linearity of Proportional Counter Systems in Electron Probe X-Ray Microanalysis." Advances in X-ray Analysis*. pp. 208–220 Boston, MA: Springer.

Kato T, *et al.* (2018). Pseudo-fixed dead time circuit for designing and implementation of JEOL-type X-ray counting systems. *Chem Geol* **484**, 16–21. https://doi.org/10.1016/j.chemgeo.2017.12.030

Rémond G, *et al.* (1996). *Intensity Measurement of Wavelength Dispersive X-Ray Emission Bands: Applications to the Soft X-Ray Region*. Vienna: Springer.

Ruark AE & Brammer FE (1937). The efficiency of counters and counter circuits. *Phys Rev* **52**(4), 322. https://doi.org/10.1103/PhysRev.52.322

Schiff LI (1936). Statistical analysis of counter data. *Phys Rev* **50**(1), 88. https://doi.org/10.1103/PhysRev.50.88

Willis MJ & Montague GA (1993). Auto-tuning PI (D) controllers with artificial neural networks. *IFAC Proceedings Volumes* **26**(2), 141–144. https://doi.org/10.1016/S1474-6670(17)48441-2

Appendix

Details of the Poisson Monte Carlo Modeling

The program works with four parameters: the number of steps simulated (n), a constant time interval (T) corresponding to the time length of each step, in seconds, the count rate (N) of emitted photons reaching the detector, in count per seconds, and the detector dead time (τ), in seconds. The dead time is assumed to be nonextensible. For each step of the simulation, a time interval T_i (equals to T) is considered. Based on the count rate N and the time interval T_i, the program simulates how many photons are reaching the detector in this time interval (the total simulated time is then equals to n $*$ T). For this purpose, the cumulative distribution function (CDF) of a Poisson distribution is used. At each step, a random number is generated between 0 and 1, and the CDF is used in conjunction with this random number to determine how many photons (k) were reaching the detector in this time interval T_i.

When at least one photon reaches the detector in T_i, the total number of detected photons is increased by one (only one photon at a time is detected), and the total number of emitted photons increases by k. As a result of the detection of a photon, the detector becomes dead for a period of time corresponding to the dead time τ. The detector will then stay dead for a number of steps $j = \tau/T$. During each one of these j next steps, the program simulates how many new photons are reaching the detector. If any, these photons are not detected (because the detector is dead) but they are accounted for by the program in the number of total emitted photon. After j steps have passed, the detector is again ready for detection, and the process is repeated.

The simulations are repeated until a total of n steps are simulated. Note that for the simulations to give realistic results, the time interval T must be much smaller than the detector dead time τ (ideally 20 to 200 times smaller) and T must be a multiple of τ. By comparing the total number of detected photons with the total number of emitted photons, it is possible to determine the dead time of the detector.

Excel spreadsheet of results for 1, 2, 3, and 10 μs dead time constant values is contained in: “Comparison different correction formulas_1, 2, 3 and 10 usec.xlsx”.

Source code of the Poisson Monte Carlo Modeling is contained in a zip file “Deadtime calculations.zip”.